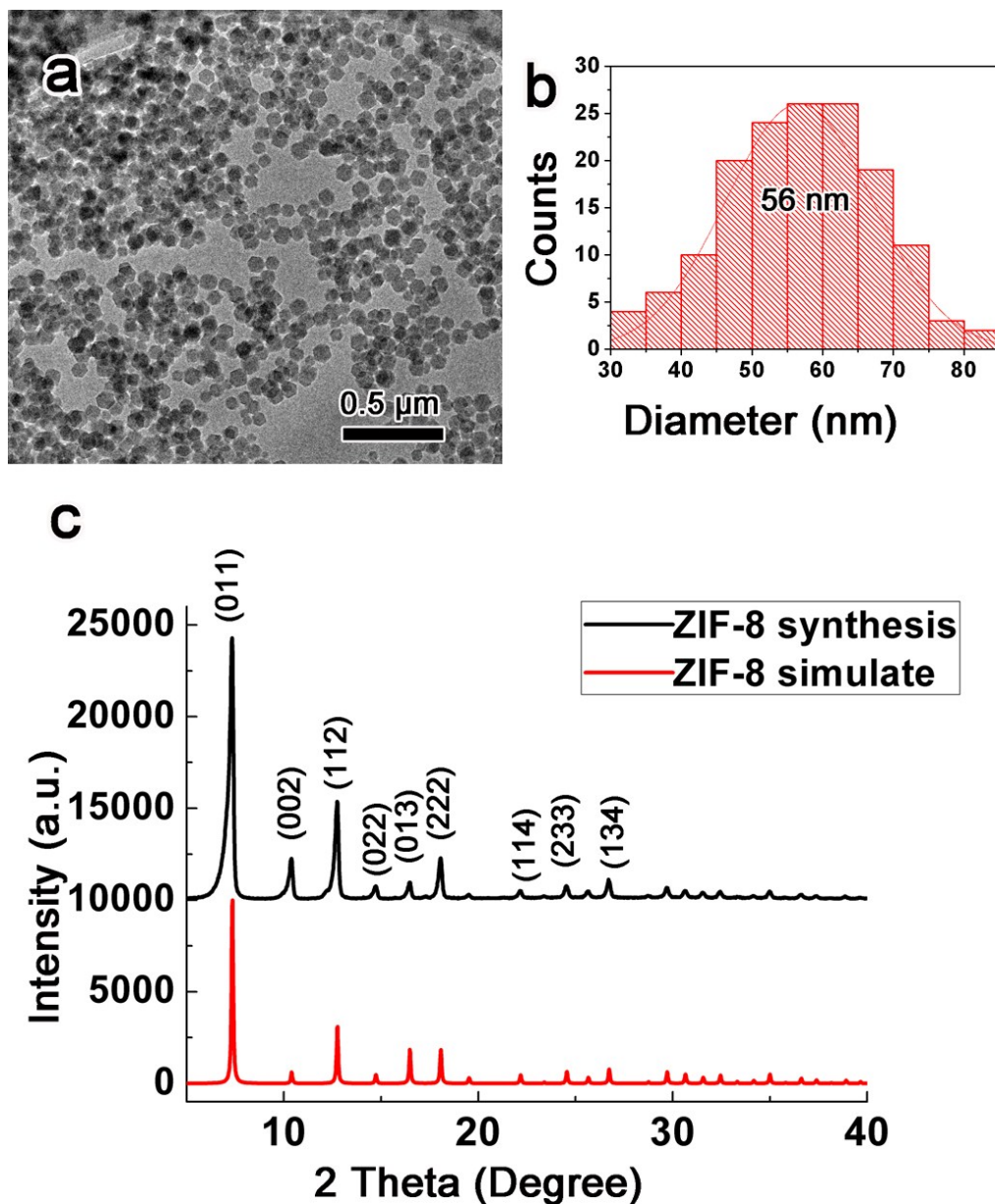


## Supporting Information

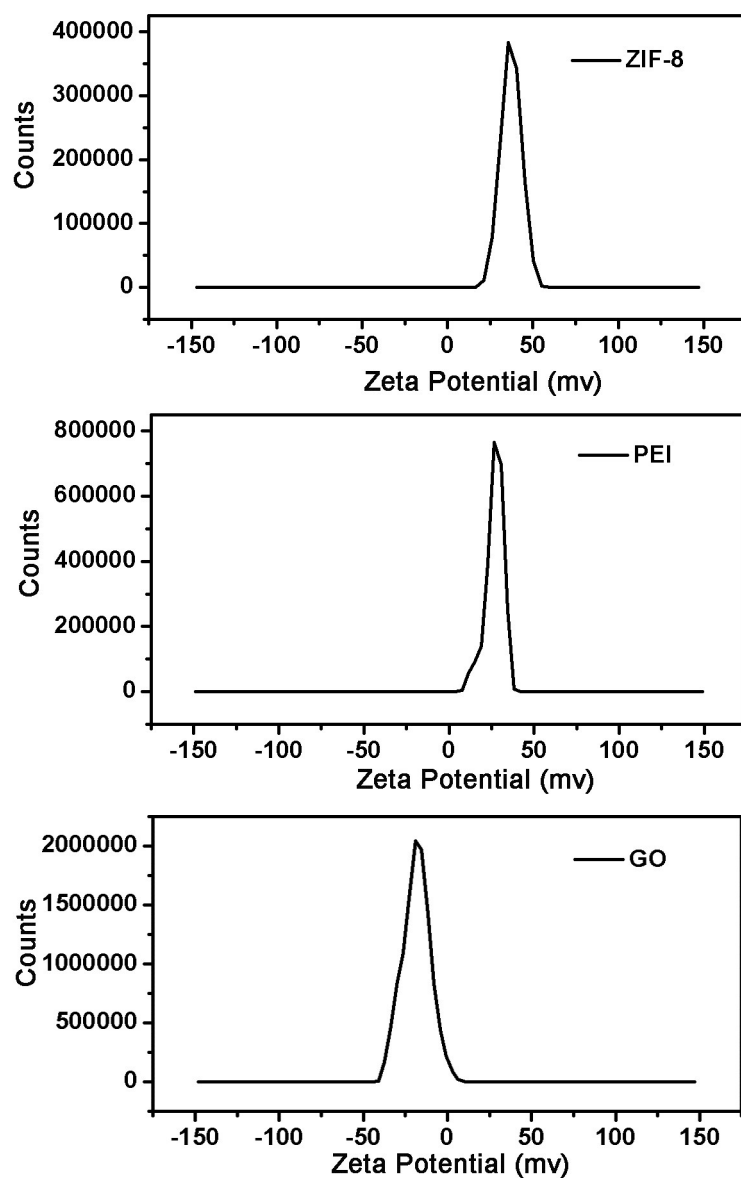
### **Interfacial Engineering of Metal-Organic Frameworks /Graphene Oxide Composite Membrane by Polyethyleneimine for Efficient H<sub>2</sub>/CH<sub>4</sub> Gas Separation**

Di Liu <sup>a,b</sup>, Guangsheng Pang<sup>\*a</sup>, Zhiyong Tang<sup>\*b</sup> and Shouhua Feng<sup>a</sup>



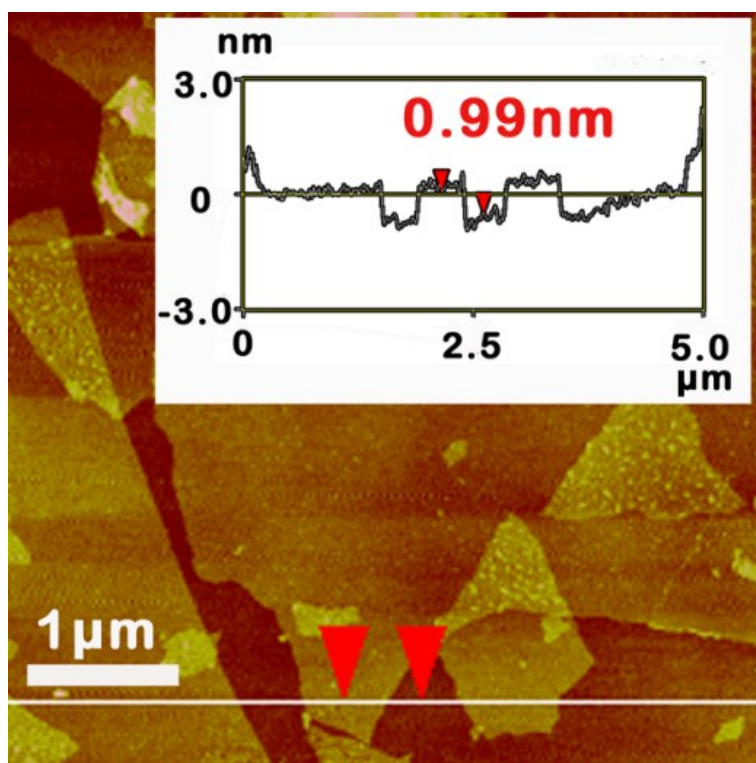
**Figure S1.** a) Transmission electron microscope (TEM) image of as-synthesized ZIF-8 nanocrystals. b) Size distribution of as-synthesized ZIF-8 nanocrystals evaluated by their TEM images. c) Powder X-ray diffraction (XRD) pattern of as-synthesized ZIF-8 nanocrystals and simulated ZIF-8 ones (Materials Studio).

As shown in Figure S1a and S1b, as-synthesized ZIF-8 nanocrystals have a uniform size of ~56 nm. Figure S1c indicates that the synthesized nanocrystals can be indexed to ZIF-8 without any impure crystal phases.

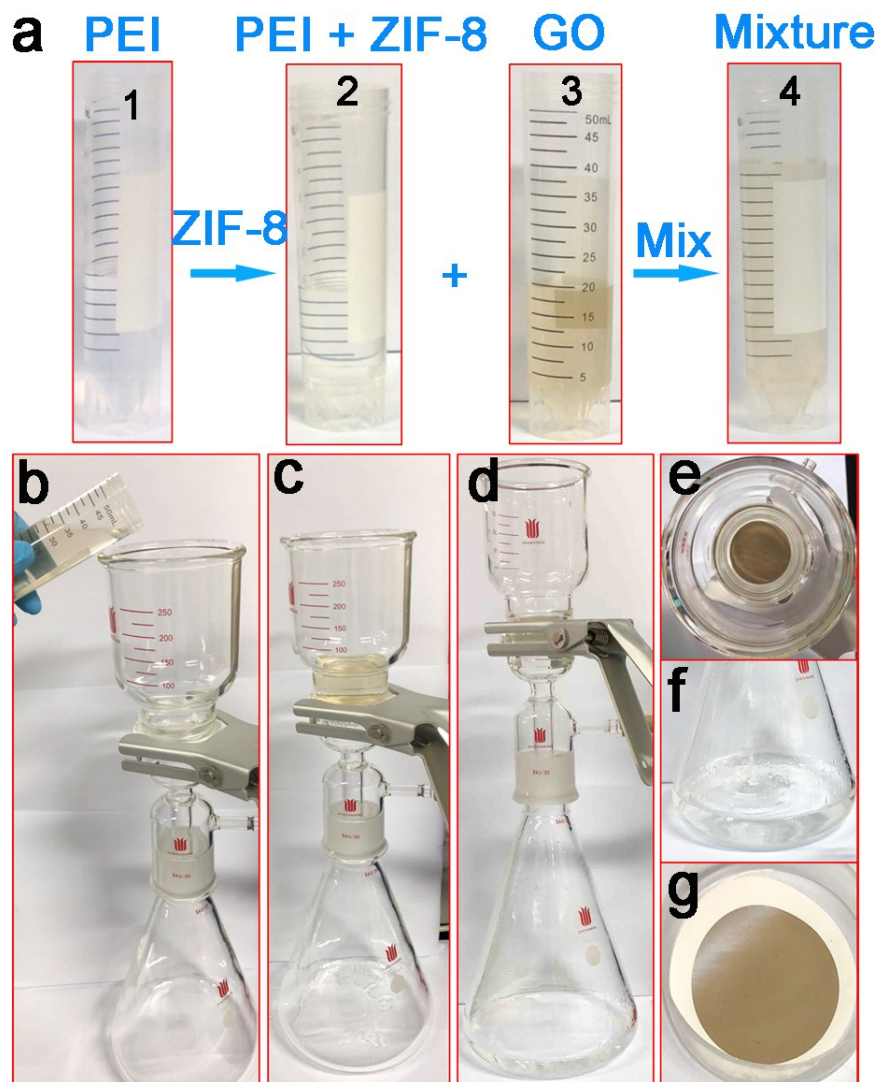


**Figure S2.** Zeta potential distribution of ZIF-8 (top), PEI (middle) and GO (bottom).

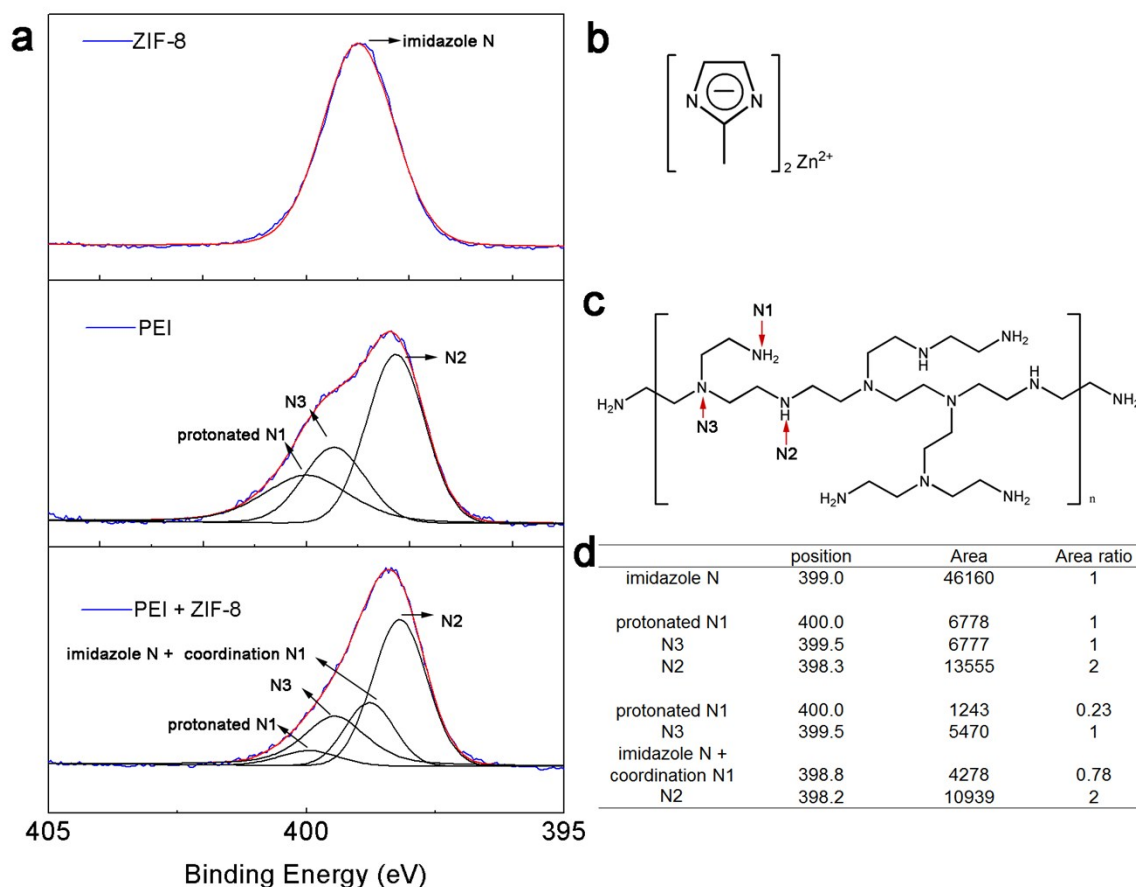
As shown in Figure S3, PEI polyelectrolytes and ZIF-8 nanocrystals are positively charged, whereas GO nanosheets are negatively charged. The exact values are summarized at Table S1.



**Figure S3.** Atomic force microscope (AMF) image of as-exfoliated GO nanosheets. Inset discloses that the thickness of nanosheets is 0.99 nm, demonstrating their monolayer nature.

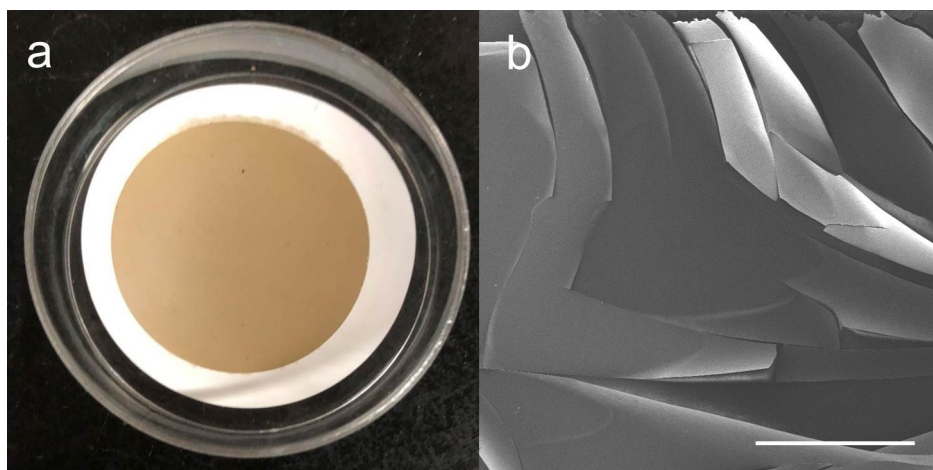


**Figure S4.** a) Preparation of the mixture solution: solution 1 (PEI) is added with ZIF-8 solution to make solution 2 (PEI + ZIF-8), and solution 2 is mixed with solution 3 (GO) to make the mixture solution 4; b) adding the above mixture solution 4; c) filtration process; d) after filtration; e) top view of as-formed membrane; f) the filtered solution; g) the obtained gas membrane after drying.



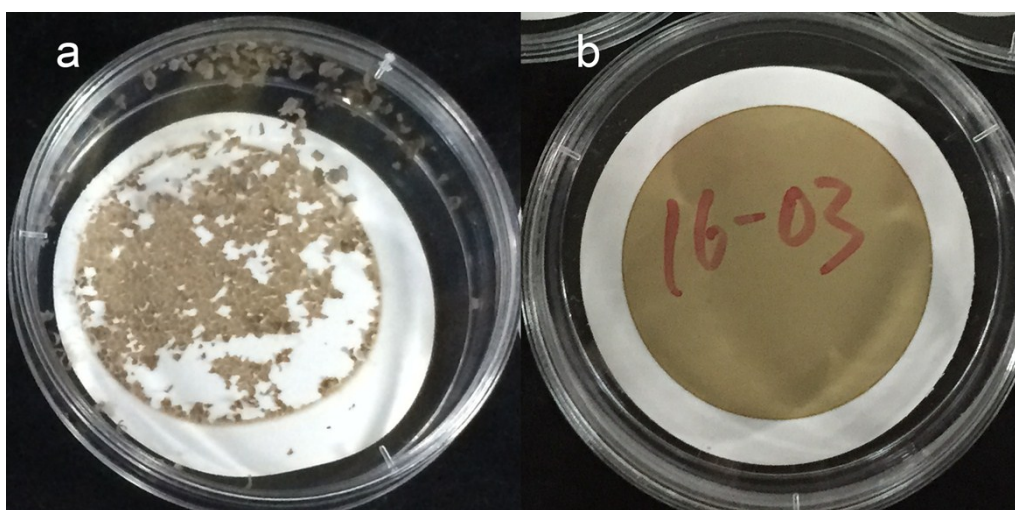
**Figure S5.** a) X-ray photoelectron spectroscopy (XPS) of ZIF-8, PEI, and mixture of ZIF-8 and PEI. The N environment of b) ZIF-8 c) PEI. d) Table of XPS position and area ratio.

In regard of ZIF-8, two N atoms in imidazole are equivalent because of its conjugated structure (Figure S5b). As for branched PEI, the N has three types of chemical environment according to the chemical formula, and N1, N2 and N3, respectively, stand for the primary, secondary and tertiary amine (Figure S5c). Theoretically, the atomic ratio of N1: N2: N3 is 1: 2: 1, which is consistent with the experimental measurement by XPS (Figure S5d). Notably, after mixing PEI with ZIF-8, the intensity of peak N1 at 400.0 eV corresponding to the protonated primary amine dramatically decreases, whereas the intensity of peak N2 at 398.2 eV and N3 at 399.5 eV remains almost unchanged (Figure S5d). Based on the literature<sup>1</sup>, the additional peak at 398.8 eV in ZIF-8 + PEI should be ascribed to both N in imidazole and the coordinated N1 in PEI. In other word, partial primary amines in PEI coordinate with Zn<sup>2+</sup> ions in ZIF-8, resulting in the decreased peak intensity at 400.0 eV.



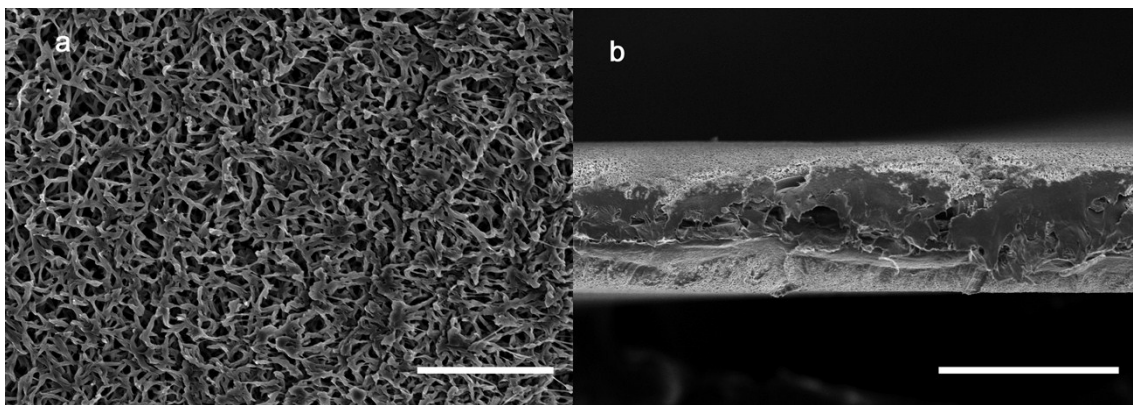
**Figure S6.** a) Photo image of the linear PEI/GO/ZIF-8 membrane. b) SEM image of the linear PEI/GO/ZIF-8 membrane's pieces. The scale bar is 1mm.

We do the contrast test of linear PEI. The membrane is well-defined (Figure S6a). However, the membrane became crisp after suffering shear force (Figure S6b). The reasons as follows: The same as branched PEI, linear PEI is positive charge. The chemical formula of linear polyethyleneimine (PEI) is  $-\text{HN}-[\text{CH}_2\text{CH}_2\text{NH}-]_n$ . From its constitutional unit, we know linear PEI is positive charge because of secondary amine. This positive charge of PEI lead to connection with GO. However, linear PEI has a very weak connection with ZIF-8 compared with branched PEI. In other words, linear PEI can connect GO, but not ZIF-8. So, the linear PEI membrane looks well outside, but fragile inside.



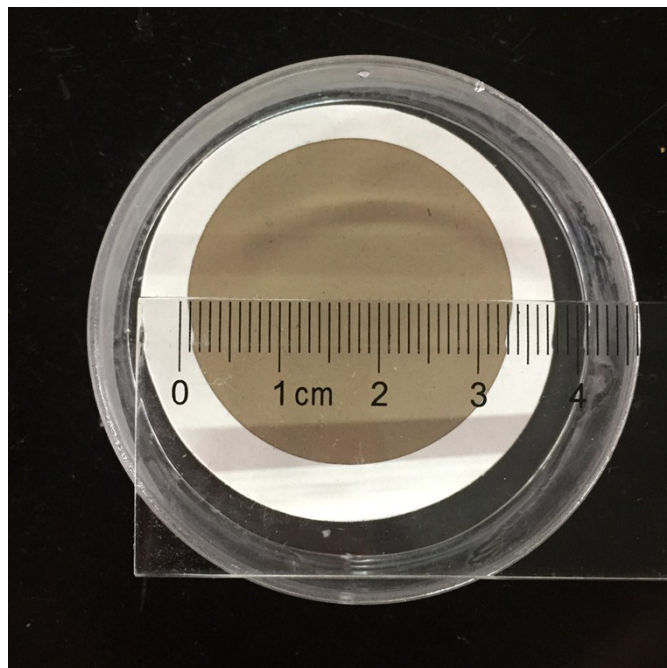
**Figure S7.** Photo images of membranes with a) no PEI adding and b) PEI adding, which are both formed on Nylon 66 polymer via filtration.

Figure S7 highlights the key role of PEI on formation of uniform and complete membranes.



**Figure S8.** a) Top view and b) cross section of commercially-available Nylon 66 membranes. Scale bar is 10  $\mu\text{m}$  (a) and 100  $\mu\text{m}$  (b), respectively.

As displayed in Figure S8, the average pore size and thickness of commercially-available Nylon 66 membranes is 0.22  $\mu\text{m}$  and 100  $\mu\text{m}$ , respectively.



**Figure S9.** Photo image of as-constructed membrane with ruler.

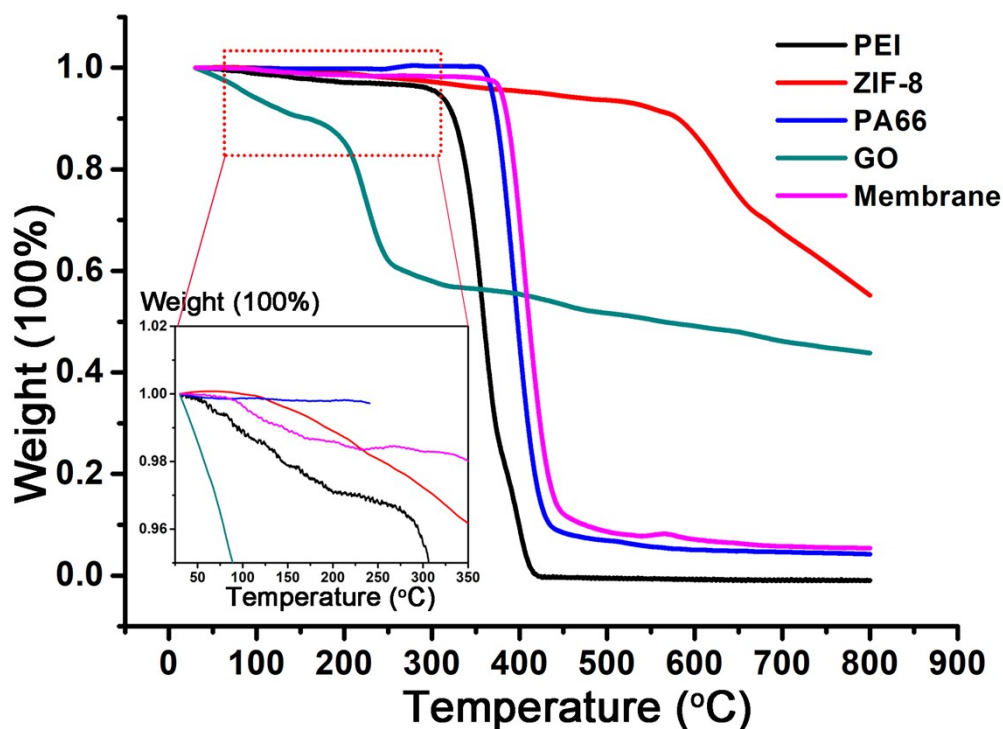
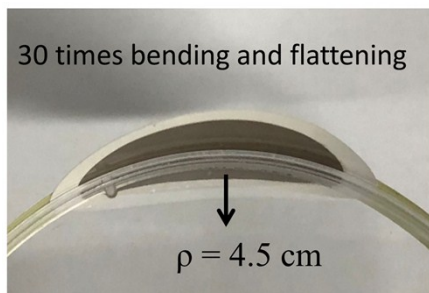


**Figure S10.** Thermogravimetric analysis (TGA) curve of PEI, ZIF-8, PA66, GO and membrane, in which the original adding ratio of ZIF-8 to GO is 1.0. Inset is the magnification of curves in the low temperature part.

The TGA curve of composite membrane (pink) shows the same inflection point temperature with GO (green) and ZIF-8 (red) at  $\sim 190^{\circ}\text{C}$  and  $\sim 580^{\circ}\text{C}$ , respectively, confirming existence of GO and ZIF-8. Generally, the weight loss of GO, PEI, PA-66, and ZIF-8 occurs mainly in the temperature range of  $190^{\circ}\text{C} - 250^{\circ}\text{C}$ ,  $300^{\circ}\text{C} - 410^{\circ}\text{C}$ ,  $360^{\circ}\text{C} - 430^{\circ}\text{C}$ , and  $580^{\circ}\text{C} - 800^{\circ}\text{C}$ , respectively. Based on the TGA data, one can quantitatively estimate the ratio of ZIF-8/GO in the composite membranes (detailed calculation in Table S2). Note that the measured mass ratio of ZIF-8/GO in the membrane is 1.2, similar to adding mass ratio of 1.0 in the precursor solution.



Radius of Curvature ( $\rho$ )	Permeance [ $10^{-8} \text{ mol m}^{-2} \text{ s}^{-1} \text{ Pa}^{-1}$ ]	Selectivity
4.5 cm	6.3	43

**Figure S11.** Membrane gas separation performance after 30 times bending experiment.

To examine the robustness, the membrane is subjected to 30 times bending and flattening, followed by gas separation experiment (Figure S10). It is clear that both the permeance and selectivity remain unchanged, disclosing the mechanic robustness of the composite membranes.

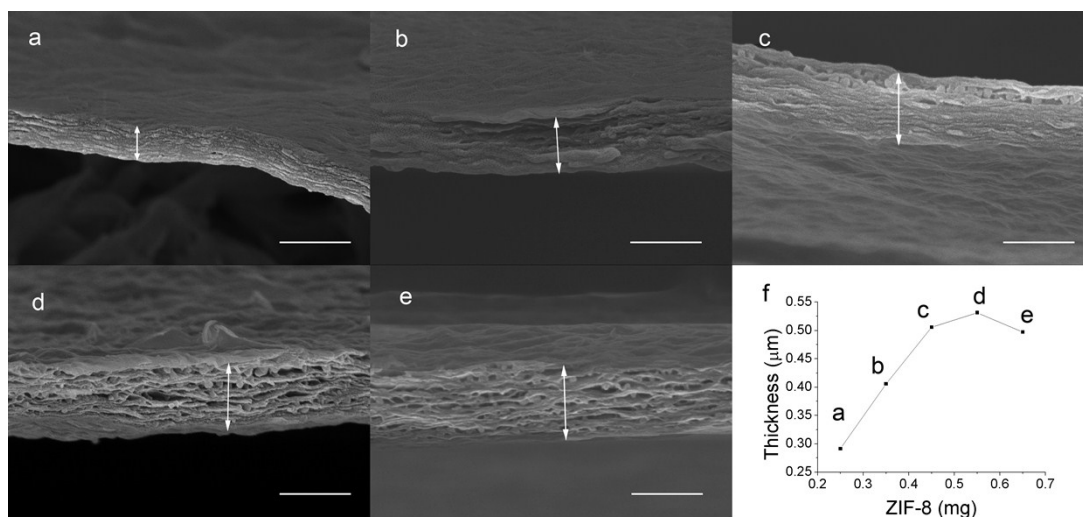


**Figure S12.** a-e) SEM images of the cross-section of membranes constructed with different adding amount of ZIF-8. As for membrane a to e, the adding amount of ZIF-8 nanocrystals is 0.25 mg, 0.35 mg, 0.45 mg, 0.55 mg and 0.65 mg, respectively. The scale bar is 500 nm. f) Relationship of membrane thickness with adding amount of ZIF-8.

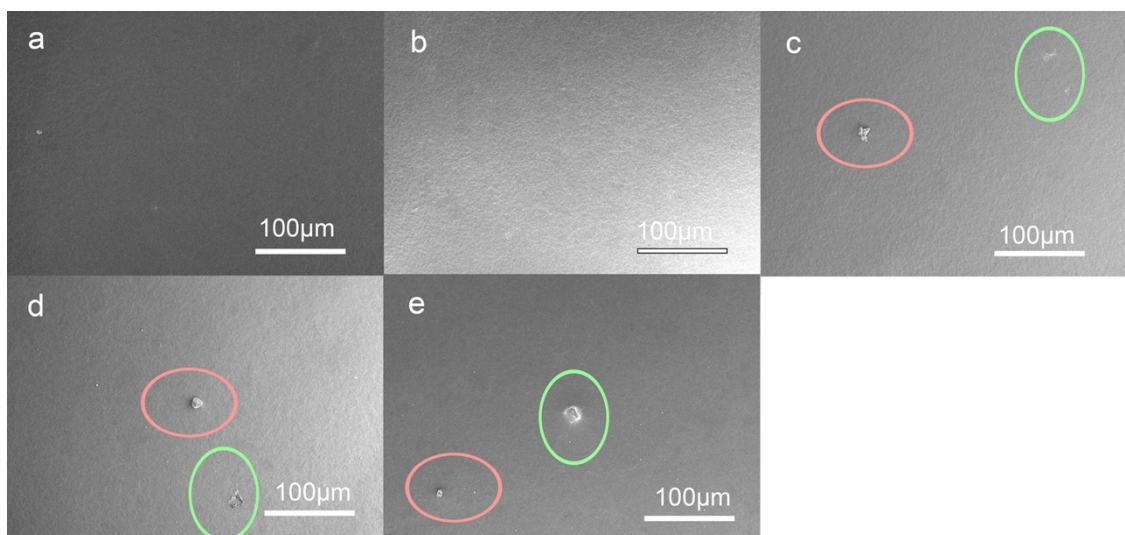


**Figure S13.** a-e) SEM images of the surfaces of membranes constructed with different adding amount of ZIF-8. As for membrane a to e, the adding amount of ZIF-8 nanocrystals is 0.25 mg, 0.35 mg, 0.45 mg, 0.55 mg and 0.65 mg, respectively. The red circles present the large particles, while the green circles show the defects.

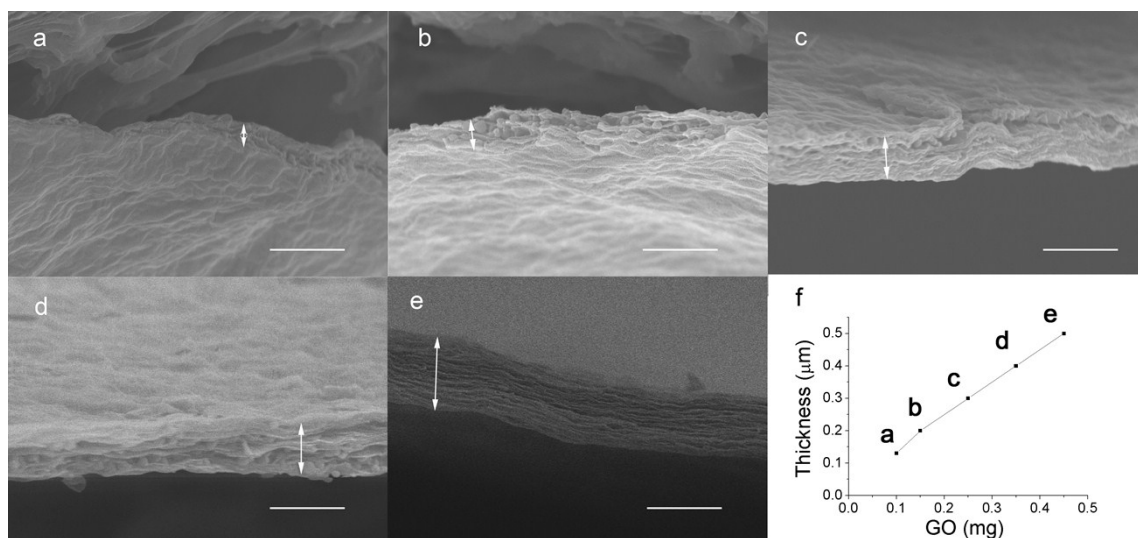


**Figure S14.** a-e) SEM images of the cross-section of membranes constructed with different adding amount of GO. As for membrane a to e, the adding amount of GO nanosheets is 0.10 mg, 0.15 mg, 0.25 mg, 0.35 mg and 0.45 mg, respectively. The scale bar is 500 nm. f) Relationship of membrane thickness with adding amount of GO.

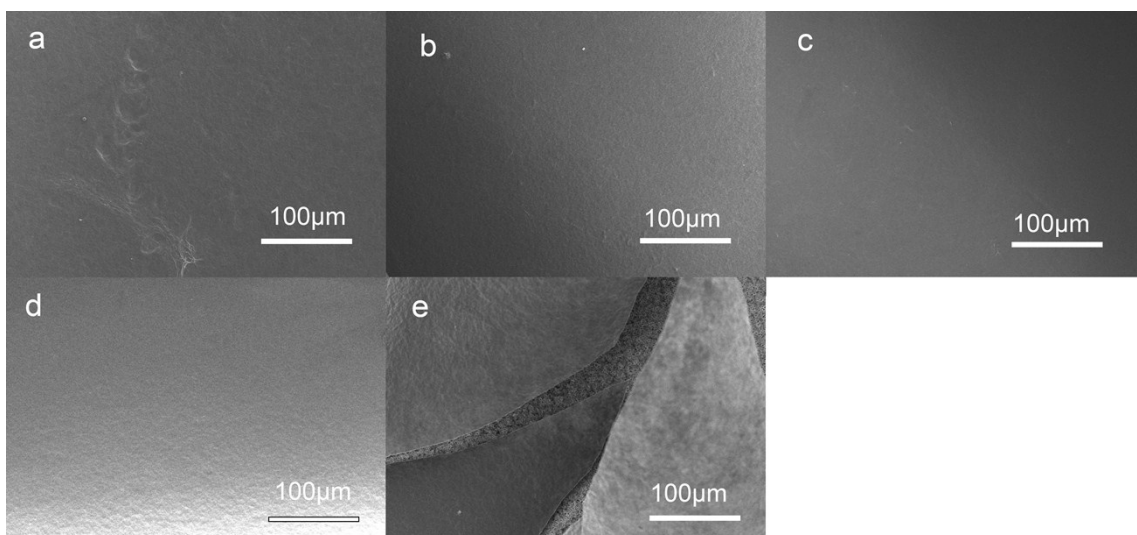


**Figure S15.** a-e) SEM images of the surfaces of membranes constructed with different adding amount of GO. As for membrane A to E, the adding amount of GO nanosheets is 0.10 mg, 0.15 mg, 0.25 mg, 0.35 mg and 0.45 mg, respectively.

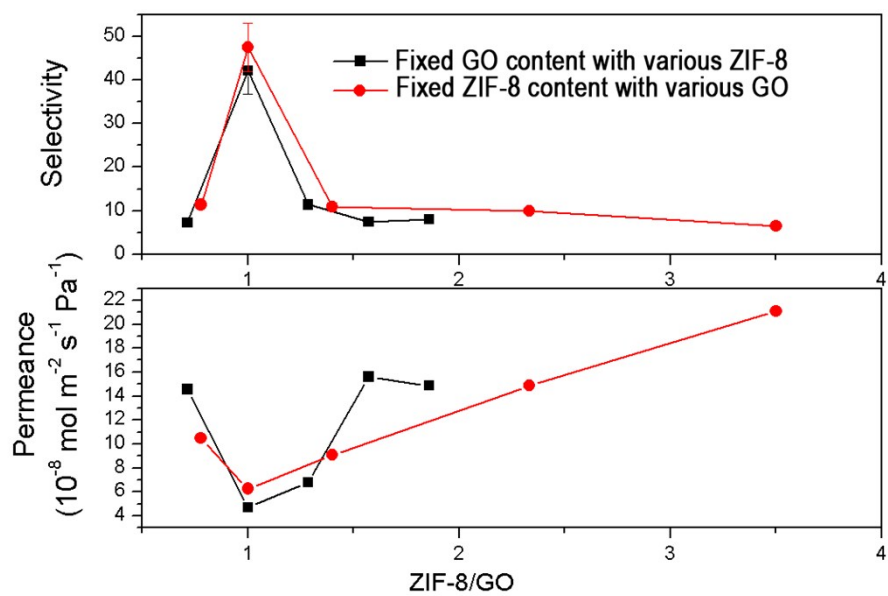


**Figure S16.** Dependence of selectivity and permeance on ZIF-8/GO mass ratio.

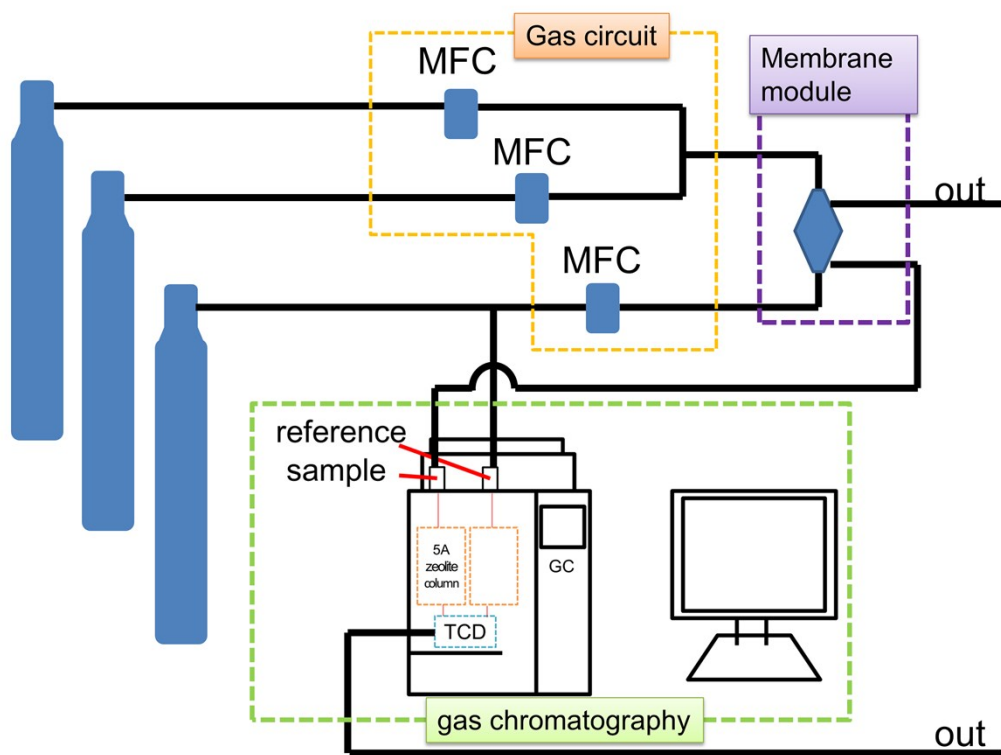


**Figure S17.** Scheme of gas selectivity and permeance measurement. MFC stands for mass flow controller, while GC represents gas chromatography.

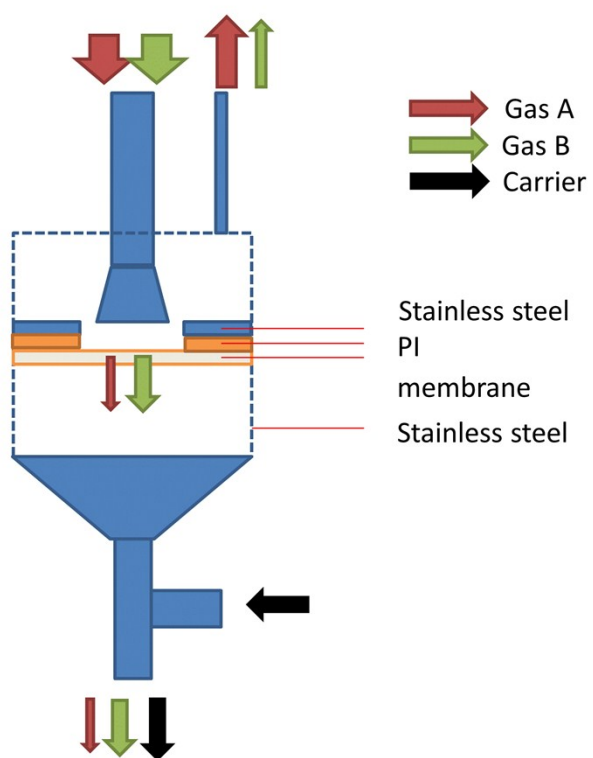


**Figure S18.** Scheme of gas flow in membrane module.

**Table S1.** Zeta potential of different components at 25°C.

Component	Zeta Potential
	[mV]
PEI polyelectrolytes	26.8
ZIF-8 nanocrystals	37.3
GO nanosheets	-20.1

**Table S2.** TGA data at different temperatures.

Temperature [°C]	PEI (X)	ZIF-8 (Y)	PA66 (A)	GO (Z)	membrane
30	1	1	1	1	1
254	0.96819	0.98019	0.99934	0.61380	0.98399
357	0.54098	0.96050	0.99959	0.56374	0.97879
581	0	0.89996	0.05235	0.49575	0.07691
800	0	0.55197	0.04218	0.43840	0.05384

Calculation of the proportion of different components in the composite membranes:

The percentage of support PEI, ZIF-8, PA66 and GO in the composite membranes is denoted as X, Y, A and Z.

For instance, when increasing temperature from 30°C to 254°C, the weight loss of the composite membrane should originate from the weight loss of each part, shown by the bellowed equation:

$$(1 - 0.96819)X + (1 - 0.98019)Y + (1 - 0.99934)A + (1 - 0.6138)Z = 1 - 0.98399$$

Therefore, four temperature regions (30°C - 254°C, 30°C - 357°C, 30°C - 581°C, and 30°C - 800°C) are selected for solving the four parameters, namely, X, Y, A and Z.

The calculation result is: X = 0.00682, Y = 0.0325, A = 0.943, and Z = 0.0376.

Reasonably, the support PEI contributes most of weight, and the mass ratio between ZIF-8, GO and PEI is estimated to be 1.0: 1.2: 0.2.

**Table S3.** Selectivity and permeance of H<sub>2</sub> and CH<sub>4</sub> compared with other literature.

No.	Journal	Year	Test condition	thickness	H <sub>2</sub> /CH <sub>4</sub> Selectivity	H <sub>2</sub> Permeance [10 <sup>-8</sup> mol m <sup>-2</sup> s <sup>-1</sup> Pa]	Material
1	JACS <sup>2</sup>	2009	25°C/1 bar	40 μm	11.2	6.8	ZIF-8
2	JACS <sup>3</sup>	2013	150°C/1 bar	20 μm	31.5	19	ZIF-8
3	JACS <sup>4</sup>	2014	25°C/1 bar	20 μm	12	14	ZIF-8
4	JACS <sup>5</sup>	2014	25°C/1 bar	20 μm	30.3	2.1	ZIF-8 @ GO
5 <sup>a</sup>	Angew. <sup>6</sup>	2016	25°C/1 bar	100 nm	11	5.5	ZIF-8 @ GO
our work			25°C/1 bar	400 nm	42	6.3	ZIF-8 @ GO

<sup>a</sup>ideal selectivity

## Reference

1. D. Li, *Surface Technology*, 2010, **39**, 24.
2. H. Bux, F. Y. Liang, Y. S. Li, J. Cravillon, M. Wiebcke, J. Caro, *J. Am. Chem. Soc.*, 2009, **131**, 16000.
3. Q. Liu, N. Wang, J. Caro, A. Huang, *J. Am. Chem. Soc.*, 2013, **135**, 17679.
4. Y. Liu, N. Wang, J. H. Pan, F. Steinbach, J. Caro, *J. Am. Chem. Soc.*, 2014, **136**, 14353.
5. A. Huang, Q. Liu, N. Wang, Y. Zhu, J. Caro, *J. Am. Chem. Soc.*, 2014, **136**, 14686.
6. Y. X. Hu, J. Wei, Y. Liang, H. C. Zhang, X. W. Zhang, W. Shen, H. T. Wang, *Angew. Chem. Int. Ed.*, 2016, **55**, 2048.